

Oxidation of Thioglycolate by $[\text{Os}(\text{phen})_3]^{3+}$: an Unusual Example of Redox-Mediated Aromatic Substitution

Meiling Hung and David M. Stanbury*

Department of Chemistry, Auburn University, Auburn, Alabama 36849

Received July 25, 2005

The aqueous oxidation of thioglycolic acid (TGA) by $[\text{Os}(\text{phen})_3]^{3+}$ (phen = 1,10-phenanthroline) is catalyzed by traces of ubiquitous Cu^{2+} and inhibited by the product $[\text{Os}(\text{phen})_3]^{2+}$. In the presence of dipicolinic acid (dipic), which thoroughly masks trace Cu^{2+} catalysis, and spin trap PBN, the kinetics under anaerobic conditions have been studied in the pH range 1.82–7.32. The rate law is $-\text{d}[\text{Os}(\text{phen})_3]^{3+}/\text{dt} = k[\text{TGA}]_{\text{tot}}[\text{Os}(\text{phen})_3]^{3+}$, with $k = 2\{(k_b K_{a1} + k_c K_{a1} K_i)[\text{H}^+] + k_d K_{a1} K_{a2}\} / \{[\text{H}^+]^2 + K_{a1}[\text{H}^+] + K_{a1} K_{a2}\}$; K_{a1} and K_{a2} are the successive acid dissociation constants of TGA, and K_i is the tautomerization constant of two TGA monoanions. $k_b + k_c K_i = (5.9 \pm 0.3) \times 10^3 \text{ M}^{-1} \text{ s}^{-1}$, $k_d = (1.6 \pm 0.1) \times 10^9 \text{ M}^{-1} \text{ s}^{-1}$ at $\mu = 0.1 \text{ M}$ (NaCF_3SO_3) and 25°C . The major products in the absence of spin traps are dithiodiglycolic acid, $[\text{Os}(\text{phen})_3]^{2+}$, and $[\text{Os}(\text{phen})_2(\text{phen-tga})]^{2+}$, where phen-tga is phenanthroline with a TGA substituent. A mechanism is proposed in which neutral TGA is unreactive, the (minor) thiolate form of the TGA monoanion undergoes one-electron oxidation by $[\text{Os}(\text{phen})_3]^{3+}$ (k_c), and the dianion of TGA likewise undergoes one-electron oxidation by $[\text{Os}(\text{phen})_3]^{3+}$ (k_d). The Marcus cross relationship provides a good account for the magnitude of k_d in this and related reactions of TGA. $[\text{Os}(\text{phen})_2(\text{phen-tga})]^{2+}$ is suggested to arise from a post-rate-limiting step involving attack of the TGA $^{\bullet}$ radical on $[\text{Os}(\text{phen})_3]^{3+}$.

Introduction

Oxidations of aliphatic thiols by typical outer-sphere reagents in aqueous media would be expected to yield the corresponding thiyl radicals as intermediates, but such reactions are generally catalyzed by impurity levels of copper ions. We have recently reported the first kinetic studies of such reactions in which the copper catalysis is thoroughly inhibited.^{1–3} In two of these studies, the thiol was thioglycolic acid (TGA), with the oxidants being $[\text{IrCl}_6]^{2-}$ and $[\text{Mo}(\text{CN})_8]^{3-}$,^{2,3} while in the third study, the thiol was cysteine and the oxidant was $[\text{Mo}(\text{CN})_8]^{3-}$.¹ In all three of these reactions, the rate law is first-order in thiol, first-order in oxidant, and has a complex pH dependence, indicating rate-limiting electron transfer from the thiolate forms to the oxidants. Despite this kinetic uniformity, the products differ in each case: The TGA/Ir reaction gives a mixture of the disulfide and the sulfonic acid,³ the TGA/Mo reaction yields only the disulfide,² and the cysteine/Mo reaction yields a

mixture of the disulfide and the sulfinic acid.¹ Moreover, the two TGA studies require significantly different thiyl/thiolate self-exchange rate constants in order to comply with the Marcus cross relationship.

In an effort to probe the factors leading to the differing product mixtures and the differing effective self-exchange rate constants, we now report on the oxidation of TGA by $[\text{Os}(\text{phen})_3]^{3+}$, which differs by being a cation and has an E° intermediate between $[\text{IrCl}_6]^{2-}$ and $[\text{Mo}(\text{CN})_8]^{3-}$. The results demonstrate yet another class of reaction product, in this case obtained by thiyl radical attack on the coordinated phen ligand, and they help clarify the variability in the effective self-exchange rate constants.

Experimental Section

Reagents and Solutions. Sodium thioglycolate, 2,6-pyridinedicarboxylic acid (dipicolinic acid) (dipic), *N-tert*-butyl- α -phenylnitron (PBN), 1,2-dibromoethane ($\text{C}_2\text{H}_4\text{Br}_2$), and 1,10-phenanthroline (phen) were used as received from Aldrich Chemicals Co. Osmium tetroxide (Sigma), Br_2 , and CH_3CN (Fisher) were used without further purification. 5,5-Dimethyl-1-pyrroline *N*-oxide (DMPO, Aldrich) was purified by microdistillation under vacuum.⁴ Triflic acid (3M Chemicals Co.), $\text{CF}_3\text{SO}_3\text{H}$, was distilled under reduced pressure in $\text{N}_2(\text{g})$; the diluted distillate was then standard-

* Corresponding author. E-mail: stanbmd@mail.auburn.edu.

- (1) Hung, M.; Stanbury, D. M. *Inorg. Chem.* **2005**, *44*, 3541–3550.
- (2) Saha, B.; Hung, M.; Stanbury, D. M. *Inorg. Chem.* **2002**, *41*, 5538–5543.
- (3) Sun, J.; Stanbury, D. M. *J. Chem. Soc., Dalton Trans.* **2002**, 785–791.

ized before use in reactions. Sodium triflate was prepared by slowly adding sodium carbonate to triflic acid and cooling in an ice bath with vigorous stirring; the product was collected and recrystallized from H_2O at 80–85 °C. CD_3CN (Cambridge Isotope Lab) and D_2O (Aldrich) were used as solvents for NMR experiments. 3-(Trimethylsilyl)-1-propanesulfonic acid, sodium salt (DSS) (Aldrich) was used as the NMR standard reference. Sulfoacetic acid ($\text{HO}_3\text{-SCH}_2\text{CO}_2\text{H}$), technical grade, and dithiodiglycolic acid ($\text{HO}_2\text{CH}_2\text{-SSCH}_2\text{CO}_2\text{H}$) from Aldrich were used without purification to spike NMR samples. Dithiodiglycolic acid for the kinetic studies was recrystallized from acetone at 45 °C.

Solutions of HClO_4 (Fisher) and $\text{CF}_3\text{SO}_3\text{H}$ were quantified by standardized NaOH solution. $\text{CF}_3\text{SO}_3\text{Na}$ stock solution was run through a cation-exchange column packed with Dowex 50W-X8 resin and then quantified with standardized $\text{NaOH}(\text{aq})$. TGA was standardized iodometrically; to avoid the over-oxidation that would occur during direct iodometric standardization of TGA,⁵ stock TGA solutions were diluted to ~0.01 M, treated with a known excess of 0.03 M I_3^- , and then back-titrated with standardized thiosulfate. TGA solutions were prepared freshly with dipic and spin trap (PBN or DMPO) in buffer solution. Solutions of $[\text{Os}(\text{phen})_3]^{3+}$ were prepared by addition of a deficiency of $\text{Br}_2/\text{CH}_3\text{CN}$ to $[\text{Os}(\text{phen})_3]^{2+}$, in situ in 1 mM triflic acid or acidic buffer right before reaction.⁶ Selected buffers (acetate, citrate, monochloroacetate, cacodylate, and hydrogen phosphate buffers) were applied to maintain pH. All TGA and $[\text{Os}(\text{phen})_3]^{3+}$ solutions were purged with Ar or N_2 prior to reaction to prevent potential complications caused by O_2 .^{7–9} All solutions were prepared in deionized water obtained from a Barnstead NANO pure Infinity ultrapure water system.

Preparation of Strontium Sulfinoacetate. 1,2-Bis(carboxymethylsulfonyl)ethane was prepared from TGA and $\text{C}_2\text{H}_4\text{Br}_2$ following the method of Reuterskiold.¹⁰ There are two signals at chemical shifts of 4.32(s) and 3.94(s) ppm in the ^1H NMR spectrum of the product. Those peaks are assigned to the methylene groups (3.94(s) ppm) between two sulfonyl groups and the other methylene groups (4.32(s) ppm) between the sulfonyl and the carbonyl groups. 1,2-Bis(carboxymethylsulfonyl)ethane was converted to $\text{Sr}(\text{O}_2\text{CCH}_2\text{-SO}_2)$ following the procedure reported by Rohde and Senning.¹¹ The ^1H NMR spectrum (Figure S-1 in Supporting Information) of $\text{Sr}(\text{O}_2\text{CCH}_2\text{SO}_2)$ at pH 7.9 displays a singlet at 3.24(s) ppm assigned to the methylene protons; the compound is not very stable in acidic media. Further support for the identification of this material comes from negative-ion electrospray ionization mass spectrometry (ESIMS) (Figure S-2 in Supporting Information), which shows a strong signal at $m/z = 123$ with two isotopic peaks at 124 and 125 corresponding to $\text{HO}_2\text{CCH}_2\text{SO}_2^-$.

Preparation of $[\text{Os}(\text{phen})_3](\text{CF}_3\text{SO}_3)_2$. The starting materials $(\text{NH}_4)_2\text{OsCl}_6$ and K_2OsCl_6 were prepared from OsO_4 by the method of Dwyer and Hogarth.¹² $[\text{Os}(\text{phen})_3]\text{Cl}_2$ was prepared by a modification of literature procedures.^{13,14} A mixture of 0.116 g of

1,10-phenanthroline and 0.097 g of K_2OsCl_6 in 15 mL of ethylene glycol (the reducing agent and the solvent) was refluxed with constant stirring at ~200 °C for 5 h. The viscous product mixture was filtered through a nylon membrane (45 μm) to remove $\text{KCl}(\text{s})$, and the residues were rinsed with a minimum volume of ethylene glycol and then washed with acetone. Ethylene glycol and excess phenanthroline in the filtrate were extracted ($\times 8$) into an ether/acetone (4:1, v/v) mixture, leaving a fine black precipitate of $[\text{Os}(\text{phen})_3]\text{Cl}_2$ as the crude product. With $(\text{NH}_4)_2\text{OsCl}_6$ as starting material, no filtration was needed prior to extraction.

$[\text{Os}(\text{phen})_3]\text{Cl}_2$ was converted to its tetrafluoroborate salt by adding saturated NaBF_4 dropwise to 60 mg of the chloride salt in minimum volume of H_2O . A dark gray precipitate was recovered. To increase its solubility, the BF_4^- salt was converted to the triflate salt. This BF_4^- salt (82 mg) was dissolved in 12 mL of H_2O at 60 °C with constant stirring, and then 2 mL of 1.16 M $\text{CF}_3\text{SO}_3\text{H}$ was added dropwise. Yield: 75 mg. Anal. Calcd for $[\text{Os}(\text{phen})_3](\text{CF}_3\text{-SO}_3)_2 \cdot \text{H}_2\text{O}$: C, 44.36%; H, 2.35%; N, 8.17%. Found: C, 44.55%; H, 2.56%; N, 8.17%. In a subsequent synthesis, $[\text{Os}(\text{phen})_3](\text{CF}_3\text{-SO}_3)_2$ was directly prepared from the crude chloride salt after extraction by adding 5 mL of 1.24 M triflic acid. The recovered triflate salt was dissolved in a minimum volume of water at 60 °C and then precipitated with 10 mL of 1.24 M triflic acid. Yield: 66%. The ^1H NMR spectrum (Figure S-3 in Supporting Information) shows four signals at 7.580(dd), 8.059(d), 8.265(s), and 8.423(d) ppm representing the four unique protons of D_3 $[\text{Os}(\text{phen})_3]^{2+}$. The UV–vis spectrum (Figure S-4 of Supporting Information) gives the extinction coefficient of $[\text{Os}(\text{phen})_3]^{2+}$ as $1.85 \times 10^4 \text{ M}^{-1} \text{ cm}^{-1}$ at 430 nm, which agrees with $1.9 \times 10^4 \text{ M}^{-1} \text{ cm}^{-1}$.⁶ The cyclic voltammetry (CV) shows a reversible wave (Figure S-5 in Supporting Information) with $E_{1/2} = 634 \text{ mV}$ vs Ag/AgCl , and the Osteryoung square wave voltammogram (OSWV) (Figure S-6 in Supporting Information) shows a single peak with $E_p = 644 \text{ mV}$. The positive-ion ESIMS spectrum (Figure S-7, Supporting Information) shows a strong parent-ion signal at $m/z = 365.6$ with an isotopic pattern in good agreement with the simulated pattern.

Methods. Electrochemical measurements were performed on a BAS 100B electrochemical analyzer equipped with a BAS C3 cell stand with purging and stirring system; cells were constructed with a glassy carbon disk working electrode, a $\text{Ag}/\text{AgCl}(\text{s})$ reference electrode ($E^\circ = 0.205 \text{ V}$ vs NHE),¹⁵ and Pt wire auxiliary electrode in 0.1 M NaCl . A Corning model 450 pH/ion meter with a Mettler Toledo InLab 421 pH electrode was used for pH measurement. ^1H NMR spectra were obtained with Bruker AC 250 and AV 400 spectrometers.

Spectrophotometric titrations for stoichiometry determination was performed on a Hewlett-Packard 8453 diode-array spectrophotometer equipped with a 1-cm rectangular quartz cuvette adapted for N_2 purge and a Brinkmann BMS Lauda thermostat to maintain temperature at 25.0 ± 0.1 °C. They were monitored at 430 nm with a 375-nm cutoff optical filter to minimize the photoinduced decompositions of $[\text{Os}(\text{phen})_3]^{3+}$ and DMPO.¹⁶ In a typical titration, 1.8 mL of one reactant was introduced into the N_2 -purged cuvette and then the titrant solution was added through a septum via a gastight microliter syringe with constant stirring.

Electrospray mass spectra of reactants and products were obtained with a VG Trio 2000 quadrupolar mass spectrometer equipped with an electrospray apparatus, included electrospray injection unit and control unit with MassLynx version 2.1 software.

- (4) Ohkuma, T.; Kirino, Y.; Kwan, T. *Chem. Pharm. Bull.* **1981**, *29*, 25–28.
 (5) Danehy, J. P.; Oester, M. Y. *J. Org. Chem.* **1967**, *32*, 1491–1495.
 (6) Sarala, R.; Rabin, S. B.; Stanbury, D. M. *Inorg. Chem.* **1991**, *30*, 3999–4007.
 (7) Klementova, S.; Wagnerova, D. M. *Chim. Oggi* **1991**, *9*, 27–32.
 (8) Wlodek, L. *Pol. J. Pharmacol.* **2002**, *54*, 215–223.
 (9) Zhang, X.; Zhang, N.; Schuchmann, H.-P.; von Sonntag, C. *J. Phys. Chem.* **1994**, *98*, 6541–6547.
 (10) Reuterskiold, J. A. *Chemical Abstracts* **1940**, *34*, 18250.
 (11) Rohde, M.; Senning, A. *Sulfur Rep.* **1993**, *14*, 391–413.
 (12) Dwyer, F. P.; Hogarth, J. *Inorg. Synth.* **1957**, *5*, 207.
 (13) Vining, W. J.; Caspar, J. V.; Meyer, T. J. *J. Phys. Chem.* **1985**, *89*, 1095–1099.
 (14) Zhang, C.; Haruyama, T.; Kobatake, E.; Aizawa, M. *Anal. Chim. Acta* **2000**, *408*, 225–232.

- (15) Sawyer, D. T.; Sobkowiak, A.; Roberts, J. L. *Electrochemistry for Chemists*, 2nd ed.; John Wiley and Sons: New York, 1995; p 192.
 (16) Chignell, C. F.; Motten, A. G.; Sik, R. H.; Parker, C. E.; Reszka, K. *Photochem. Photobiol.* **1994**, *59*, 5–11.

For kinetic studies, reactions were conducted by mixing equal volumes of the two reactants on a Hi-Tech Scientific model SF-51 stopped-flow mixer equipped with an SU-40 spectrophotometer, 1-cm optical cell, and a C-400 recirculating water bath. The recirculating bath was purged with N_2 throughout the sampling system. All apparent rate constants were the average of three or four reproducible runs. Other calculations were processed by KaleidaGraph 3.0.5 and Prism 4 version 4.0a software packages. All reaction solutions were purged with Ar or N_2 , transferred by airtight syringes, and contacted only glass, platinum, or Teflon before reactions. All reactions were performed in a dark room and monitored at 430 nm, 25.0 ± 0.1 °C.

Ellman's reagent was used to determine the consumption of TGA.¹⁷ In a typical analysis, the analyte solution was diluted appropriately and then treated with Ellman's reagent, 5,5'-dithiobis-(2-benzoic acid) (DTNB), with constant stirring for about 10 min to complete the thiol exchange reaction. The mixture was then analyzed spectrophotometrically.

Product Separation and Identification. Tests for the products arising from TGA were performed by 1H NMR spectroscopy. A product solution was prepared from 1.99 mM TGA and 1.32 mM $[Os(phen)_3]^{3+}$ in the presence of 1.53 mM dipic and 1.53 mM DSS in D_2O . The pH of the solution after reaction was 2.46. Resonances were assigned by spiking the solution with authentic samples of TGA, sulfoacetic acid, dithiodiglycolic acid, and strontium sulfinoacetate.

Osmium-containing products were identified by performing a macroscale reaction with 30 mg of $[Os(phen)_3]^{2+}$ converted to $[Os(phen)_3]^{3+}$ by bromine oxidation. A gastight syringe was used to deliver 1 mL of a solution containing 0.046 M TGA and 22 mM dipic to 24.5 mL of $[Os(phen)_3]^{3+}$ solution under $N_2(g)$. The product solution was then loaded onto a cation-exchange column packed with Sephadex SP-C25. The column was eluted with progressively increasing concentrations of HCl from 0.05 to 0.5 M. Two dark bands eventually separated, were collected, and taken to dryness by rotary evaporation. The first band was identified as $[Os(phen)_3]^{2+}$ by its 1H NMR spectrum. The second band has a 1H NMR spectrum (Figure S-8) with a complex pattern of at least seven resonances in the aromatic region and a singlet at 4.02 ppm. A second preparation of the product mixture performed with twice the concentration of TGA yielded the same two bands by chromatography. The first band gave an OSWV (Figure S-9), a UV-vis spectrum (Figure S-10), and a positive-ion ESIMS spectrum (data not shown), all consistent with its identification as $[Os(phen)_3]^{2+}$. The second band gave an OSWV with an oxidation peak at 612 mV vs Ag/AgCl(s) (Figure S-9), a UV-vis spectrum with a peak at 437 nm (Figure S-10), and a positive-ion ESIMS spectrum with a peak at $m/z = 411.0$ (Figure S-11), all consistent with its identification as $[Os(phen)_2(phen-tga)]^{2+}$.

Results

TGA is a diprotic acid with pK_{a1} and pK_{a2} of 3.48 and 10.11, respectively, at 0.1 M ionic strength.¹⁸ These two acid/base equilibria are established rapidly on the time scale of the experiments described below, and thus we designate the total concentration of TGA in its various protonation states as $[TGA]_{tot}$.

(17) Garman, A. J. *Nonradioactive Labeling*; Academic Press: San Diego, 1997; p 119.

(18) Martell, A. E.; Smith, R. M.; Motekaitis, R. J. *NIST Critically Selected Stability Constants of Metal Complexes Database, 7.0*; U.S. Department of Commerce: Gaithersburg, MD, 2003;

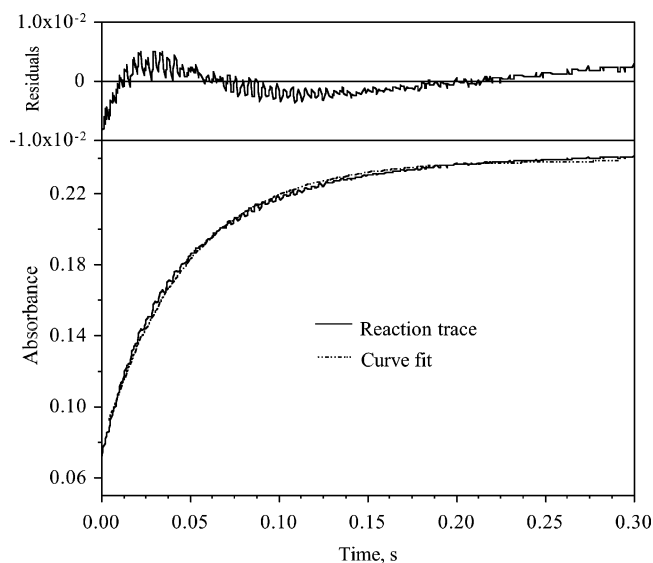


Figure 1. A kinetic trace of the oxidation of TGA by $[Os(phen)_3]^{3+}$ demonstrating deviations from pseudo-first-order kinetics: 1.10×10^{-3} M TGA, 8.88×10^{-6} M $[Os(phen)_3]^{3+}$ with 5.72×10^{-6} M $[Os(phen)_3]^{2+}$, 1 mM dipic at pH 4.63 (acetate buffer), $\mu = 0.1$ M ($NaCF_3SO_3$) and 25 °C, monitored at 430 nm in the absence of PBN with curve fit and residuals. k_{obs} is 22.2 s $^{-1}$.

Metal-Ion Catalysis. Tests for catalysis by Ni^{2+} , Mn^{2+} , Zn^{2+} , Co^{2+} , Fe^{3+} , and Cu^{2+} of the oxidation of TGA by $[Os(phen)_3]^{3+}$ were performed with and without the presence of 1×10^{-5} M metal ions. These experiments were performed with $[TGA]_{tot} = 7.5 \times 10^{-4}$ M and 1.26×10^{-5} M $[Os(phen)_3]^{3+}$ at 25 °C; the pH and ionic strength were controlled at 2.87–2.89 (citrate buffer) and 0.126 M (sodium triflate). Kinetic data are summarized in Table S-1 (Supporting Information). Of the ions tested, only Cu^{2+} is significantly catalytic. It is highly catalytic, reducing the half-life to less than the dead time of the stopped-flow instrument (~ 2 ms) and thus accelerating the reaction at least 16-fold. Comparative reactions with no additional metal ion were performed in the absence and presence of 1 mM dipic, which we have previously used as an inhibitor of copper catalysis.^{1,2} As shown in Table S-1, dipic slows the reaction by a factor of 12.5, indicating that impurity levels of Cu^{2+} dominate the kinetics when inhibitors are absent. The capability of dipic to mask Cu^{2+} catalysis was further examined at pH 4.5 (0.01 M acetate buffer) as summarized in Table S-2 (Supporting Information). With no additional Cu^{2+} and dipic, a reaction with $[TGA]_{tot} = 7.6 \times 10^{-4}$ M and 1.46×10^{-5} M $[Os(phen)_3]^{3+}$ had a 5 ms half-life, and upon addition of 1×10^{-5} M Cu^{2+} , the reaction rate was too fast to be detected. In the presence of 1 mM dipic, the half-lives were 45 ms with or without additional Cu^{2+} , and the same results were obtained in the presence of 2 mM dipic. Thus, 1 mM dipic completely blocks catalysis by adventitious metal ions. All further experiments described below utilize dipic as an inhibitor to probe the direct oxidation of TGA by $[Os(phen)_3]^{3+}$.

Kinetic Effects of $[Os(phen)_3]^{2+}$ and PBN/DMPO. Figure 1 shows a typical kinetic trace for the reaction of $[Os(phen)_3]^{3+}$ with a large excess of TGA at pH 4.6 (with

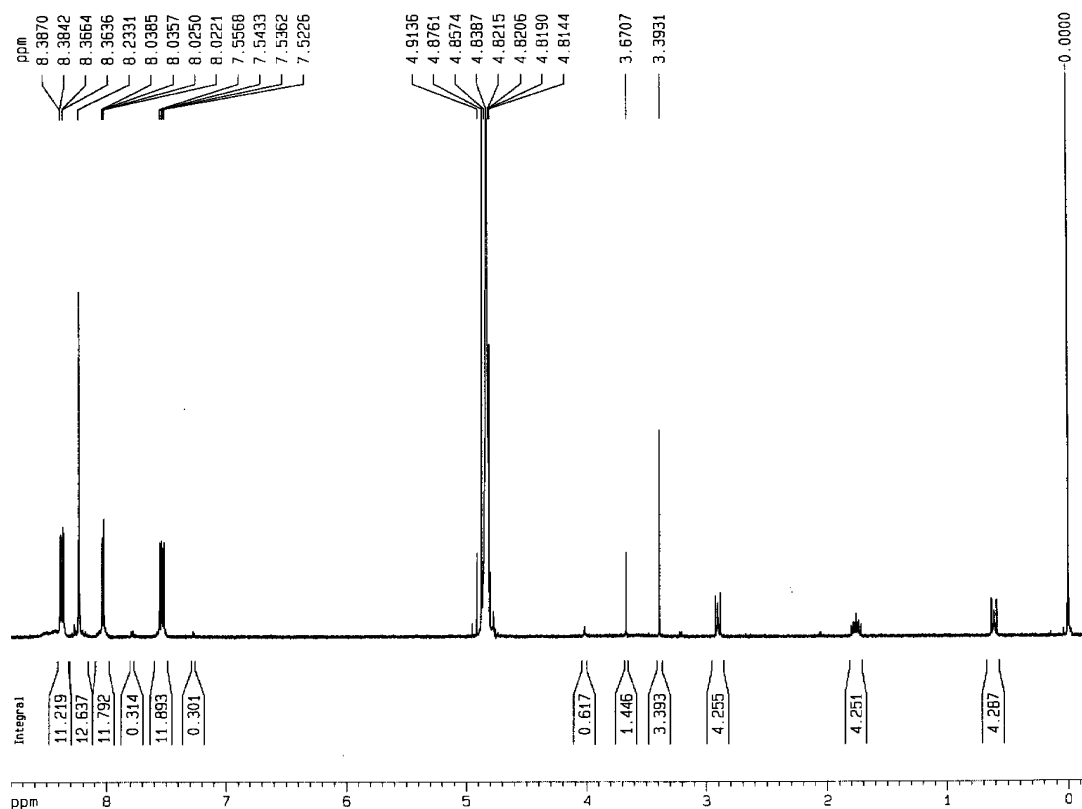


Figure 2. The ^1H NMR spectrum of the oxidation of 1.99 mM TGA by 1.32 mM $[\text{Os}(\text{phen})_3]^{3+}$ with 1.53 mM dipic and 1.53 mM DSS in D_2O at pH 2.46. According to the integration, $[\text{RSH}] = 1.22$ mM $[\text{RSSR}] = 0.26$ mM and $[\text{Os}(\text{phen})_2(\text{phen-tga})^{2+}] = 0.22$ mM (from the $-\text{CH}_2-$ group at 4.02 ppm).

dipic as an inhibitor of copper catalysis), and it shows small but significant deviations from pseudo-first-order kinetics suggestive of product inhibition. Accordingly, the following experiment was performed to test for the effect of $[\text{Os}(\text{phen})_3]^{2+}$, which is a reaction product. As a reference, the half-life was 0.13 s for a reaction with $[\text{TGA}]_{\text{tot}} = 2.50 \times 10^{-4}$ M and 6.95×10^{-6} M $[\text{Os}(\text{phen})_3]^{3+}$ in the presence of 2.27×10^{-6} M $[\text{Os}(\text{phen})_3]^{2+}$ and 1 mM dipic at pH 4.63 (0.02 M acetate buffer), $\mu = 0.1$ M ($\text{CF}_3\text{SO}_3\text{Na}$) at 25 °C; for a similar reaction performed in the presence of 4.18×10^{-5} M $[\text{Os}(\text{phen})_3]^{2+}$, the half-life increased to 0.21 s.

If it is assumed that the observed inhibition by Os(II) is due to reversible electron transfer from TGA to Os(III), then it is reasonable to propose that scavenging of the TGA radicals would eliminate the product inhibition and yield good pseudo-first-order kinetics. In agreement with this hypothesis, when 1 mM spin-trap PBN is introduced into the reaction mixture under the conditions of Figure 1, the half-life is reduced from 0.13 to 0.102 s with excellent pseudo-first-order kinetics (see Figure S-12, Supporting Information). Thus, the addition of PBN at pH 4.6 increases k_{obs} by a factor of 1.3. The effect of spin traps DMPO and PBN on the reaction at pH 5 with $[\text{TGA}]_{\text{tot}} = 1.9 \times 10^{-4}$ M, 1.01×10^{-5} M $[\text{Os}(\text{phen})_3]^{3+}$, and 1 mM dipic is identical; excellent pseudo-first-order behavior is observed, with $k_{\text{obs}} = 22.4$ s $^{-1}$ for the reaction with 1 mM PBN and $k_{\text{obs}} = 22.5$ s $^{-1}$ for that with 1 mM DMPO. A series of oxidations of TGA by $[\text{Os}(\text{phen})_3]^{3+}$ was conducted with various concentrations of PBN at pH 2.94 in the presence

of 1 mM dipic, at ionic strength 0.08 M (sodium citrate). Values of k_{obs} are summarized in Table S-3 (Supporting Information) and indicate that the addition of 1 mM PBN at pH 2.94 doubles k_{obs} and that k_{obs} is independent of the concentration of PBN over the range of 1–5 mM.

Blank experiments show that no reaction occurs during 60 s at pH 2.95 between 3.2×10^{-5} M $[\text{Os}(\text{phen})_3]^{2+}$ and either $[\text{TGA}]_{\text{tot}} = 3.8 \times 10^{-4}$ M, 1 mM PBN, or 1 mM dipic individually or a combination with all of these ingredients. PBN reacts with $[\text{Os}(\text{phen})_3]^{3+}$ very slowly over a 60-s period at pH 4.8, but this reaction is suppressed in the presence of 1 mM dipic. Consequently, the reaction of PBN with $[\text{Os}(\text{phen})_3]^{3+}$ can be neglected during the reaction of TGA with $[\text{Os}(\text{phen})_3]^{3+}$. Another potential complication is the direct reaction of TGA with the spin traps. This reaction has been reported to occur between TGA and the spin trap DEPMPO, with an equilibrium constant of 0.14 M $^{-1}$;¹⁹ with such a low equilibrium constant, the reaction would consume a negligibly small fraction of the TGA in the present studies. In view of the effectiveness of PBN in suppressing product inhibition, all of the following kinetic studies were performed with 1 mM PBN.

RSSR Effect. A test was performed to investigate the reaction of $[\text{Os}(\text{phen})_3]^{3+}$ with dithiodiglycolic acid (RSSR), which is one of the reaction products. It was performed with 10 μM $[\text{Os}(\text{phen})_3]^{3+}$ and 120 μM RSSR in 0.02 M acetate

(19) Potapenko, D. I.; Bagryanskaya, E. G.; Tsentlovich, Y. P.; Reznikov, V. A.; Clanton, T. L.; Khramtsov, V. V. *J. Phys. Chem. B* **2004**, *108*, 9315–9324.

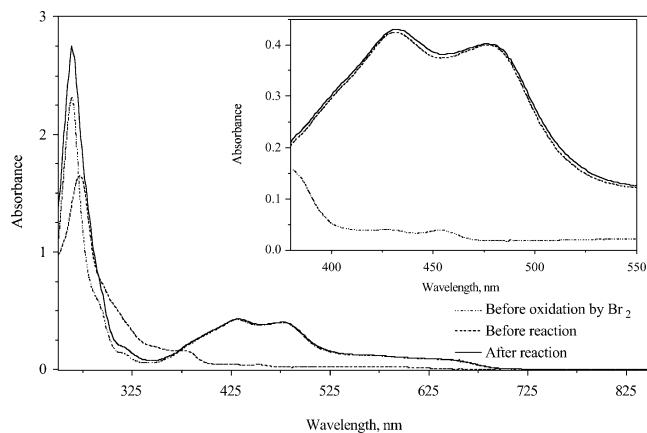


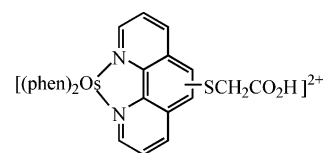
Figure 3. Overlaid UV-vis spectra of Os complex before and after oxidation by Br_2 , and after reaction with TGA. For the optical analysis, solutions were diluted to have $[\text{Os}] = 2.41 \times 10^{-5} \text{ M}$ in 0.218 mM citric acid. Both reactant solutions were purged with Ar for at least 15 min before mixing for reaction. Inset is the enlarged spectrum over the region of 380–550 nm.

buffer (pH 4.8) in the presence of 1 mM dipic and 1 mM PBN at 25 °C. Less than 10% of the $[\text{Os}(\text{phen})_3]^{3+}$ was converted to $[\text{Os}(\text{phen})_3]^{2+}$ over 80 s, indicating that RSSR is unreactive under these conditions.

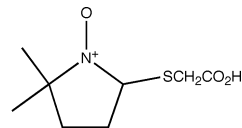
Product Identification. When PBN and DMPO were omitted from the reaction mixture at pH 2.46, the ^1H NMR spectrum (Figure 2) indicates that RSSR ($\delta = 3.67$) is the major product derived from TGA and that neither sulfoacetate nor sulfinacetate are produced in significant yields.

Careful examination of the UV-vis and ^1H NMR spectra suggests that $[\text{Os}(\text{phen})_3]^{2+}$ is the major osmium-containing product and that at least one other minor osmium-containing product is also formed. Thus, Figure 3 shows the UV-vis spectrum of the product mixture arising from the reaction of 1.21 mM $[\text{Os}(\text{phen})_3]^{3+}$ with $[\text{TGA}]_{\text{tot}} = 10 \text{ mM}$ at pH 2.98 (citrate buffer): the absorption band near 430 nm is shifted somewhat relative to the starting Os(II) spectrum. Likewise, the ^1H NMR spectrum in Figure 2 shows the production of $[\text{Os}(\text{phen})_3]^{2+}$ along with other small peaks in the aromatic region and another peak at 4.02 ppm. A product having the unique ^1H NMR resonance at 4.02 ppm was identified as being cationic through the findings that it was removed from the product mixture by passing a sample through a cation-exchange column but not removed by an anion-exchange column. Bulk cation-exchange chromatography of the product mixture led to the separation and isolation of two colored substances. One of these is easily identified as $[\text{Os}(\text{phen})_3]^{2+}$ by its characteristic UV-vis, ^1H NMR, and ESIMS spectra and OSWV properties. The other, a novel compound, was identified by the following information. Its ion-exchange properties clearly show that it is a cation. As shown in Figure S-10, its UV-vis spectrum closely resembles that of $[\text{Os}(\text{phen})_3]^{2+}$, which suggests that it is a ring-substituted derivative of $[\text{Os}(\text{phen})_3]^{2+}$. Its OSWV (see Figure S-9) is shifted 38 mV cathodically relative to that of $[\text{Os}(\text{phen})_3]^{2+}$, which is also consistent with ring substitution. Its ^1H NMR spectrum (see Figure S-8) is well-resolved but complex in the aromatic region, indicating that

the material is diamagnetic (as expected for Os(II)) and suggesting that a phen ligand has been altered by substitution at one of the peripheral sites; moreover, this compound displays a characteristic peak in the aliphatic region at 4.02 ppm, which is absent in the spectrum of $[\text{Os}(\text{phen})_3]^{2+}$. Its ESIMS positive-ion spectrum (shown in Figure S-11) has an isotopic pattern similar to that of $[\text{Os}(\text{phen})_3]^{2+}$ but shifted from $m/z = 365.6$ to $m/z = 411.0$; note that $z = 2$ for both species, so the difference in m/z corresponds to half of the TGA formula weight. These observations serve to identify this product as $[\text{Os}(\text{phen})_2(\text{phen-tga})]^{2+}$:



The products of the reaction in the presence of DMPO were examined by ^1H NMR spectroscopy (Figure 4). A sample with $[\text{TGA}]_{\text{tot}} = 2 \text{ mM}$ was oxidized by 0.98 mM $[\text{Os}(\text{phen})_3]^{3+}$ in the presence of 1.7 mM dipic in D_2O with 0.8 mM DSS at pH 3 without DMPO and with 1.8 mM DMPO. Besides the peaks attributable to $[\text{Os}(\text{phen})_2(\text{phen-tga})]^{2+}$ and RSSR in the aliphatic region, a new peak at 3.84-(s) ppm appears in the presence of DMPO. This new peak is assigned to the CH_2 group adjacent to S in



(DMPO-tga⁺), which is the oxidized spin adduct of DMPO and the TGA thiyl radical. Another experiment was conducted under essentially the same conditions but at a higher concentration of DMPO (6.47 mM). As indicated by the peak integrals, the yield of the oxidized spin adduct increased with a corresponding decrease in the yields of $[\text{Os}(\text{phen})_2(\text{phen-tga})]^{2+}$ and RSSR.

The product distribution of the reaction with PBN present was also examined by ^1H NMR. The reaction solution contained $[\text{TGA}]_{\text{tot}} = 2.51 \text{ mM}$, 1.58 mM $[\text{Os}(\text{phen})_3]^{3+}$, 8.03 mM PBN, and 4.38 mM dipic in D_2O with 8.92 mM DSS as a reference. According to the peak integrals, the yields of RSSR and $[\text{Os}(\text{phen})_2(\text{phen-tga})]^{2+}$ were about 0.2 mM for each species, and no oxidized spin-adduct was observed. An explanation for this observation could be that the reaction produces a mixture of the spin adduct and its oxidized cation and that this mixture is undetectable because of rapid electron exchange between its two components.

Stoichiometry. A semiquantitative measure of sulfur conservation for the reaction in the absence of PBN or DMPO was obtained from integration of the ^1H NMR peaks in Figure 2. The derived concentrations of TGA_{tot} , RSSR, and $[\text{Os}(\text{phen})_2(\text{phen-tga})]^{2+}$ in the product mixture are 1.22, 0.26, and 0.22 mM, respectively, which agrees with the initial concentration of TGA.

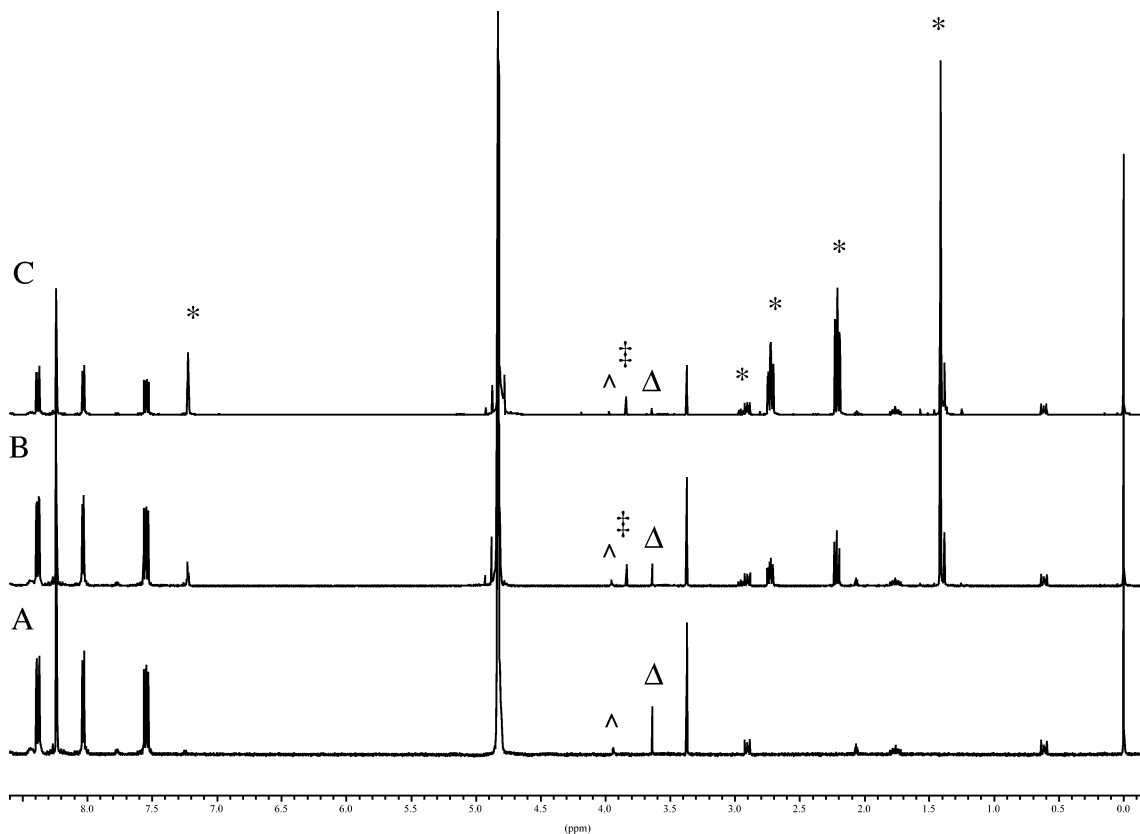
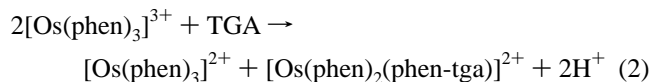
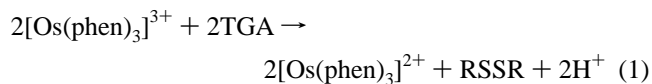


Figure 4. Stacked ^1H NMR spectra with various concentration of DMPO. Sample A: reaction solution with 2.0 mM TGA, 1.02 mM $[\text{Os}(\text{phen})_3]^{3+}$ and 1.7 mM dipic in D_2O with 0.8 mM DSS, pH 2.99 after reaction. Sample B: reaction solution with 2.0 mM TGA, 0.98 mM $[\text{Os}(\text{phen})_3]^{3+}$, 1.7 mM dipic and 1.8 mM DMPO in D_2O with 0.8 mM DSS, pH 3.01 after reaction. Sample C: 1.84 mM TGA, 1.18 mM $[\text{Os}(\text{phen})_3]^{3+}$, 0.66 mM dipic and 6.5 mM DMPO in D_2O with 1.52 mM DSS, pH 3.00 after reaction. No buffer was used in samples. †, oxidized DMPO-adduct; \wedge , $[\text{Os}(\text{phen})(\text{phen-tga})]^{2+}$; Δ , dithiodiglycolic acid; *, DMPO.

Consumption ratios were determined in one set of experiments by analysis of the TGA_{tot} concentration remaining after reaction with a deficiency of $[\text{Os}(\text{phen})_3]^{3+}$. An experiment was performed with $[\text{TGA}]_{\text{tot}} = 9.1 \times 10^{-5} \text{ M}$ and $4.4 \times 10^{-5} \text{ M}$ $[\text{Os}(\text{phen})_3]^{3+}$ in the presence of 1 mM dipic at pH 7.5. Equal volumes of reactant solutions were mixed on a stopped-flow spectrophotometer. The remaining concentration of TGA_{tot} in the product solution was assayed by use of Ellman's reagent as $6.3 \times 10^{-5} \text{ M}$, which implies a consumption ratio $n_{\text{Os(III)}}/n_{\text{TGA}}$ of 1.46. A similar experiment was performed in the presence of 1 mM PBN and 1 mM dipic, with $[\text{TGA}]_{\text{tot}} = 5.00 \times 10^{-5} \text{ M}$ and $3.49 \times 10^{-5} \text{ M}$ $[\text{Os}(\text{phen})_3]^{3+}$ at pH 6.33. The remaining concentration of TGA_{tot} was $3.27 \times 10^{-5} \text{ M}$, and thus, the consumption ratio $n_{\text{Os(III)}}/n_{\text{TGA}}$ is 2.02, significantly greater than in the absence of PBN.

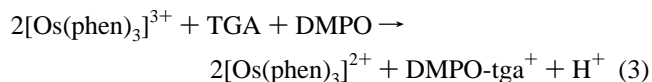
In another set of experiments, spectrophotometric titration of TGA with $[\text{Os}(\text{phen})_3]^{3+}$ was used to determine consumption ratios. Experiments were carried out in the presence of 2 mM dipic in 0.02 M acetate buffer at pH 4.9, titrating 1.8 mL of $\sim 1 \times 10^{-5} \text{ M}$ TGA_{tot} with $\sim 1 \times 10^{-4} \text{ M}$ $[\text{Os}(\text{phen})_3]^{3+}$. The consumption ratios of $n_{\text{Os(III)}}/n_{\text{TGA}}$ were 2.3 without spin trap, 1.9 with 1.9 mM DMPO, and 2.2 with 2 mM PBN. Reversed titrations of 1.8 mL of $[\text{Os}(\text{phen})_3]^{3+}$ with $3.23 \times 10^{-5} \text{ M}$ TGA_{tot} were also performed, leading to consumption ratios of 2.3 without DMPO and 1.94 with 2 mM DMPO.

The above results imply that in the absence of PBN or DMPO the overall process consists of the two parallel reactions 1 and 2.



From the consumption ratios determined at $\sim 0.1 \text{ mM}$ TGA_{tot} with Ellman's reagent at pH 7.5, these two reactions contribute 27% and 73%, respectively. Reaction 2 seems to occur almost exclusively at the much lower TGA_{tot} concentrations used in the spectrophotometric titrations at pH 4.9.

In the presence of DMPO, an additional reaction occurs:



In the presence of PBN instead of DMPO, a reaction analogous to eq 3 occurs. Under the conditions of the ^1H NMR experiments (pH ≈ 3 , $\sim 2 \text{ mM}$ TGA), all three reactions contribute significantly, while at pH 7.5 with 0.1 mM TGA_{tot} , the consumption ratios of ~ 2 indicate that reaction 1 is not a significant contributor.

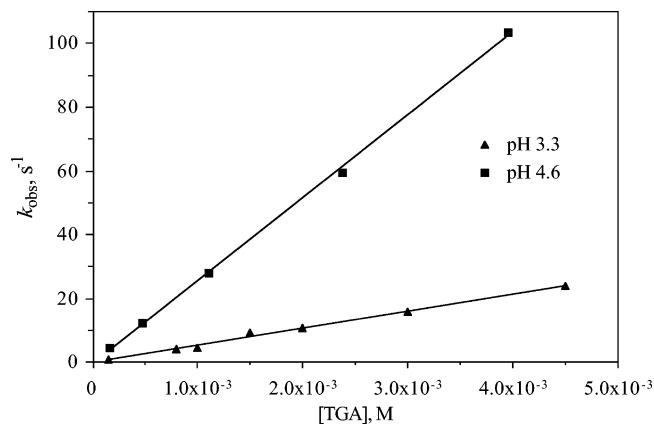


Figure 5. Plots of k_{obs} vs $[\text{TGA}]_{\text{tot}}$ at pH 3.3 (monochloroacetate buffer, \blacktriangle) and at pH 4.6 (acetate buffer, \blacksquare) in the presence of 1 mM dipic and 1 mM PBN, at $\mu = 0.1$ M (NaCF_3SO_3) and 25 °C.

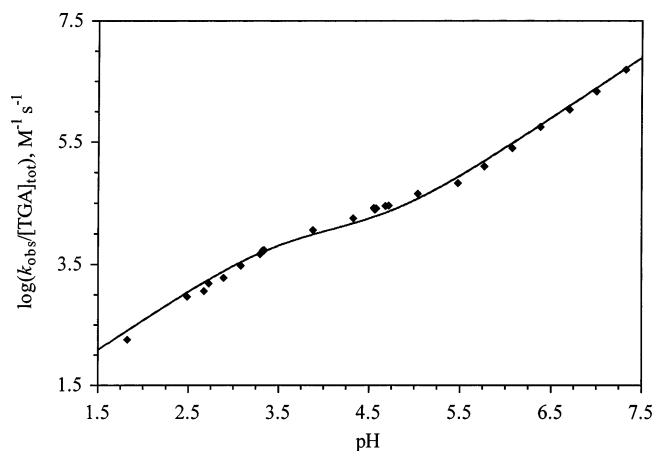


Figure 6. The plot of $\log(k_{\text{obs}}/[\text{TGA}]_{\text{tot}})$ vs pH with 1 mM dipic, 1 mM PBN, at $\mu = 0.1$ M (NaCF_3SO_3) and 25 °C. \blacklozenge represents $\log(k_{\text{obs}}/[\text{TGA}]_{\text{tot}})$ at various pH ranging from 1.82 to 7.33. Solid line is curve fit to eq 5 with K_{a1} and K_{a2} held at the literature values.

Kinetics. Under pseudo-first-order conditions, two series of oxidations of TGA by $[\text{Os}(\text{phen})_3]^{3+}$ at pH 3.3 (monochloroacetate buffer) and 4.6 (acetate buffer) were carried out with TGA concentrations $(0.15\text{--}4.5) \times 10^{-3}$ M and $(0.158\text{--}3.95) \times 10^{-3}$ M, respectively, in the presence of 1 mM dipic and 1 mM PBN at 0.1 M ionic strength (NaCF_3SO_3) and 25 °C. Kinetic data are summarized in Table S-4 (Supporting Information). The linear plots of k_{obs} vs $[\text{TGA}]_{\text{tot}}$ shown in Figure 5 with slopes $(5.34 \pm 0.19) \times 10^3 \text{ M}^{-1} \text{ s}^{-1}$ at pH 3.3 and $(2.60 \pm 0.04) \times 10^4 \text{ M}^{-1} \text{ s}^{-1}$ at pH 4.6 not only indicate that the rate law is first-order with respect to $[\text{TGA}]_{\text{tot}}$, as in

$$k_{\text{obs}} = k[\text{TGA}]_{\text{tot}} \quad (4)$$

but also show that kinetics are sensitive to pH.

The detailed effect of pH on the reaction was studied over the pH range of 1.82–7.32 with $(0.12\text{--}4.50) \times 10^{-3}$ M TGA, $(0.55\text{--}2.06) \times 10^{-5}$ M $[\text{Os}(\text{phen})_3]^{3+}$, 1 mM dipic, and 1 mM PBN at 0.1 M ionic strength ($\text{CF}_3\text{SO}_3\text{Na}$), 25 °C. Selected buffers were employed to maintain pH values. All kinetic data are collected in Table S-4. The plot of $\log(k_{\text{obs}}/[\text{TGA}]_{\text{tot}})$ vs pH shown in Figure 6 is sigmoidal with rates increasing with pH in the acid region, a narrow plateau region around pH 4.4, and then increasing again at higher pH. In

analogy with our prior studies of TGA oxidation^{2,3} we assume this behavior reflects an immeasurably low rate constant for reaction of TGA in its neutral form, a relatively small rate constant for reaction of the TGA monoanion, and a large rate constant for the dianion. Accordingly, the data have been fit with the rate law

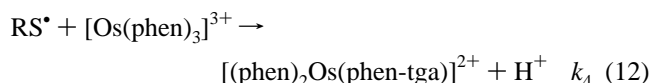
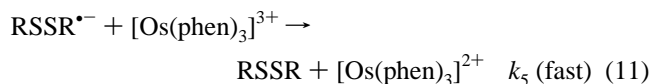
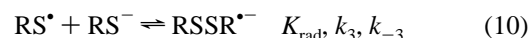
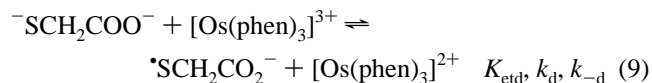
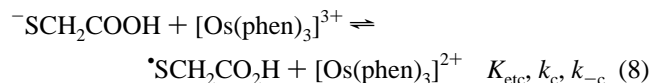
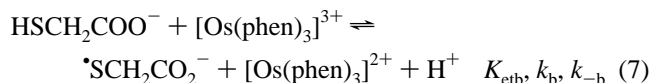
$$\frac{k_{\text{obs}}}{[\text{TGA}]_{\text{tot}}} = \frac{k'[\text{H}^+] + k''}{[\text{H}^+]^2 + K_{a1}[\text{H}^+] + K_{a1}K_{a2}} \quad (5)$$

while holding the K_{a1} and K_{a2} at their known values, 3.31×10^{-4} and 7.76×10^{-11} M, respectively.¹⁸ The resulting fit is quite adequate, as displayed in Figure 6, and the derived parameters are $k' = (3.9 \pm 0.2) \text{ s}^{-1}$ and $k'' = (8.1 \pm 0.6) \times 10^{-5} \text{ M s}^{-1}$.

Discussion

As anticipated, the oxidation of TGA by $[\text{Os}(\text{phen})_3]^{3+}$ is accelerated by traces of copper ions as are those of TGA by $[\text{IrCl}_6]^{2-}$ and $[\text{Mo}(\text{CN})_8]^{3-}$,^{2,3} and this catalysis is thoroughly inhibited by the presence of the rigid chelating ligand dipic.

The following mechanism is proposed to account for the reaction when it is conducted in the presence of dipic and no added spin traps:



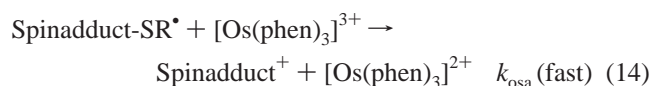
The first step this mechanism features tautomerization of the monoanionic form of TGA, for which we have previously estimated $\text{p}K_1 = \sim 7$.² The next three steps entail reversible electron transfer from the two monoanionic tautomers and the dianion of TGA to Os(III). This reversibility is invoked because of the observed kinetic inhibition by $[\text{Os}(\text{phen})_3]^{2+}$. Rapid association of the TGA[•] radical with TGA to form $\text{RSSR}^{\bullet-}$ (K_{rad}) is a well-established process.²⁰ $\text{RSSR}^{\bullet-}$ is then produced by electron transfer from $\text{RSSR}^{\bullet-}$ to $[\text{Os}(\text{phen})_3]^{3+}$, in analogy with our prior proposed mechanisms.¹⁻³ Unique to this mechanism is the final step, in which the thiyl radical

(20) Hoffman, M. Z.; Hayon, E. *J. Phys. Chem.* **1973**, *77*, 990–996.

RS[•] attacks a C–H bond of a phenanthroline ligand that is coordinated to Os(III), leading to reduction of Os(III) and displacement of the ring proton. A similar type of reductive substitution has been reported in the reaction of [Ru(NH₃)₄-(phen)]³⁺ with SO₃^{•-}.²¹

One viable alternative mechanism for the production of [(phen)₂Os(phen-tga)]²⁺ replaces reaction 12 by a two-step process, the first step being hydrogen abstraction from [Os(phen)₃]³⁺ by RS[•] to form [(phen)₂Os(phen[•])]³⁺ plus RSH, and the second step being addition of RS⁻ to [(phen)₂Os(phen[•])]³⁺. Two other alternative mechanisms for production of [(phen)₂Os(phen-tga)]²⁺ can be rejected. First, direct attack of TGA on [Os(phen)₃]²⁺ can be rejected, since incubation of these two species leads to no reaction. Second, the observed diminished yields of [(phen)₂Os(phen-SR)]²⁺ with increasing concentrations of DMPO are incompatible with production of [(phen)₂Os(phen-SR)]²⁺ through attack of TGA on [Os(phen)₃]³⁺.

In the presence of the spin traps PBN and DMPO, the above mechanism is augmented by two more steps:



Scavenging of RS[•] in the first of these steps is sufficient to eliminate kinetic inhibition by Os(II), effectively making the initial electron transfer from TGA irreversible (steps *k_b*, *k_c*, and *k_d*). By applying the steady-state approximation to all of the radical species, this augmented mechanism leads to

$$-\frac{d[\text{Os(III)}]}{dt} = \frac{2\{(k_b K_{a1} + k_c K_{a1} K_i)[\text{H}^+] + k_d K_{a1} K_{a2}\}}{[\text{H}^+]^2 + K_{a1}[\text{H}^+] + K_{a1} K_{a2}} [\text{TGA}]_{\text{tot}} [\text{Os(III)}] \quad (15)$$

Comparison of this rate law with the empirical rate law, eq 5, identifies *k'* as 2(*k_b**K_{a1}* + *k_c**K_{a1}**K_i*) and *k''* as 2*k_d**K_{a1}**K_{a2}*. Use of the literature values for *K_{a1}* and *K_{a2}* then leads to values of (5.9 ± 0.3) × 10³ and (1.6 ± 0.1) × 10⁹ M⁻¹ s⁻¹ for (*k_b* + *k_c**K_i*) and *k_d*, respectively.

The mechanism presented above allows for reactivity of both the thiolate and thiol tautomeric forms of TGA (*k_b* and *k_c*). It is reasonable to assume that only the thiolate form is reactive, since the neutral form of TGA reacts undetectably slowly. With this assumption and the use of an estimated value of 4 × 10⁻⁷ for *K_i*, the above rate constants yield a value of 1.5 × 10¹⁰ M⁻¹ s⁻¹ for *k_c*, which is at the diffusion-controlled limit for reactions of this charge type and 9-fold greater than *k_d*. Our estimate of *K_i* is based on the values for *K_{a1}* and *K_{a2}*, with the assumption that they represent the intrinsic acidities of the –COOH and –SH groups, corrected

(21) Sarala, R.; Islam, M. S.; Rabin, S. B.; Stanbury, D. M. *Inorg. Chem.* **1990**, *29*, 1133–1142.

by an interaction factor of 1.6 as seen for linear dicarboxylic acids. Given the rudimentary method for our estimation of *K_i*, the value could easily be in error by a factor of 10, and thus, it is possible that *k_c* does not exceed *k_d*. The latter outcome would be more in line with expectations on the basis of electrostatics, and in either case, the results support the concept that the Os(III) oxidizes only the thiolate forms of TGA.

We previously used a value for *E*^o for the [•]SCH₂CO₂⁻/⁻SCH₂CO₂⁻ redox couple that was derived from data with chlorpromazine as the reference redox couple.² However, it is now evident that the phenoxyl radical provides a more reliable reference potential.²² Accordingly, we use the data in Table 1 of Surdhar and Armstrong²³ to derive Δ*G*^o = 1.9 ± 1.4 kJ (or Δ*E*^o = -0.020 ± 0.14 V) for the reaction



By applying *E*^o(PhO[•]/PhO⁻) ((0.800 ± 0.010) V, determined at pH > 11)²⁴ and the dissociation constant of PhOH (p*K_a* = 9.98 ± 0.04)¹⁸ to *E*^o(PhO[•]/PhO⁻) = *E*^o(PhO[•], H⁺/PhOH) + 0.059 log *K_a*, *E*^o(PhO[•], H⁺/PhOH) and *E*^o([•]SCH₂CO₂⁻, H⁺/HSCH₂CO₂⁻) can be determined as (1.39 ± 0.01) V and (1.37 ± 0.02) V, respectively. With the p*K_{a2}* (10.61 ± 0.07, at μ = 0 M) and ionic strength correction (to μ = 0.1 M), *E_f*^o ([•]SCH₂CO₂⁻/⁻SCH₂CO₂⁻) is calculated as (0.76 ± 0.02) V.

With this *E*^o for ([•]SCH₂CO₂⁻/⁻SCH₂CO₂⁻) and our measured *E_f*^o for [Os(phen)]^{3+/2+} (=0.839 V), a value for log *K_{etd}* of 1.4 ± 0.3 is obtained. Thus, the initial electron-transfer step in the mechanism is favorable, allaying concerns that this mechanism might lead to a value for *k_{-d}* exceeding the diffusion limit. A related concern is that, with *K_{etd}* being greater than unity, how is it possible that the overall reaction displays inhibition by [Os(phen)₃]²⁺ in the absence of spin traps? The explanation is that the Os(II) inhibition was detected at pH 4.6, well below p*K_{a2}*; under such conditions, TGA is primarily in the thiol form, which leads to an unfavorable equilibrium constant for the net conversion of RSH to RS[•].

The above discussion provides strong support for description of *k_d* (= (1.6 ± 0.1) × 10⁹ M⁻¹ s⁻¹) as the rate constant for electron transfer from ⁻SCH₂CO₂⁻ to [Os(phen)₃]³⁺. Given the substitution-inert character of the oxidant, it is reasonable to anticipate that electron transfer occurs through an outer-sphere mechanism. Moreover, given that *k_d* is significantly below the diffusion-controlled limit, it is reasonable to propose that the Marcus cross relationship should be applicable to *k_d*. We use this relationship in its classical form, including work terms and the *f* factor, to derive the self-exchange rate constant (*k₁₁*) for the [•]SCH₂CO₂⁻/⁻SCH₂CO₂⁻ redox couple.^{2,25} The following parameters are used in this calculation: *k₂₂* ([Os(phen)₃]^{3+/2+}) =

(22) Armstrong, D. A. In *S-Centered Radicals*; Alfassi, Z. B., Ed.; John Wiley and Sons: New York, 1999; pp 27–61.

(23) Surdhar, P. S.; Armstrong, D. A. *J. Phys. Chem.* **1987**, *91*, 6532–6537.

(24) Das, T. N.; Huie, R. E.; Neta, P. *J. Phys. Chem. A* **1999**, *103*, 3581–3588.

$3.09 \times 10^8 \text{ M}^{-1} \text{ s}^{-1}$,²⁶ $r(\text{OsL}_3) = 6.7 \text{ \AA}$,⁶ and $r(\text{TGA}) = 2.6 \text{ \AA}$.³ With these parameters, the experimental value of k_{12} (k_d) and K_{12} (22), k_{11} is calculated as $5.3 \times 10^5 \text{ M}^{-1} \text{ s}^{-1}$. For comparison, recalculating k_{11} for the oxidations of TGA by $[\text{IrCl}_6]^{2-}$ and $[\text{Mo}(\text{CN})_8]^{3-}$ with use of our revised E° for the $\text{SCH}_2\text{CO}_2^-/\text{SCH}_2\text{CO}_2^-$ redox couple leads to effective self-exchange rates of 4.7×10^5 and $7.1 \times 10^3 \text{ M}^{-1} \text{ s}^{-1}$, respectively.^{2,3} Thus, the k_{11} values derived from the reactions of TGA with $[\text{Os}(\text{phen})_3]^{3+}$ and $[\text{IrCl}_6]^{2-}$ are in excellent agreement, while the reaction with $[\text{Mo}(\text{CN})_8]^{3-}$ is only in moderate agreement. The deviation for the Mo(V) reaction may be due to the strong electrostatic repulsion between dianionic TGA and $[\text{Mo}(\text{CN})_8]^{3-}$, a situation that is conducive to specific "inert" cation mediation. Indeed, we have previously shown that the oxidation of the dianionic form of cysteine by $[\text{Mo}(\text{CN})_8]^{3-}$ is subject to this type of cation catalysis.¹

Conclusion

Surprisingly, with this fourth study of outer-sphere thiolate oxidation (with copper catalysis inhibited) we encounter a fourth class of reaction stoichiometry. The roster includes

- (25) Zuckerman, J. J. *Inorganic Reactions and Methods*; VCH: Deerfield Beach, FL, 1986; Vol. 15, pp 13–47.
 (26) Nord, G.; Pedersen, B.; Farver, O. *Inorg. Chem.* **1978**, *17*, 2233–2238.

(1) RSSR plus RSO_3^- when TGA is oxidized by $[\text{IrCl}_6]^{2-}$,³
 (2) RSSR when TGA is oxidized by $[\text{Mo}(\text{CN})_8]^{3-}$,² (3) RSSR plus RSO_2^- when cysteine is oxidized by $[\text{Mo}(\text{CN})_8]^{3-}$,¹ and now (4) RSSR + M(L-tga) when TGA is oxidized by $[\text{Os}(\text{phen})_3]^{3+}$. Despite this diversity of products, the reactions are united in having rate laws that are first-order in oxidant and in thiolate and in having complex pH-dependent kinetics. The similarities extend to the mechanisms, where the varying product mixtures are seen to arise from differences in the post-rate-limiting steps. Some of the complexity in the product distribution is likely due to the unfavorable equilibrium constant for association of RS^* with RSH , which then allows relatively high steady-state concentrations of RS^* to develop.

Acknowledgment. This project was supported by National Science Foundation. We thank Dr. Cheng-Nan Chen (University of the Pacific) and Dr. William Hill (Auburn University) for their assistance with the mass spec experiments and Dr. Peter Livant (Auburn University) for his help with the NMR experiments.

Supporting Information Available: Tables S-1–S-4, Figures S-1–S-12. This material is available free of charge via the Internet at <http://pubs.acs.org>.

IC051241G